Mechanism for the $\alpha \rightarrow \epsilon$ phase transition in iron

Bertrand Dupé,[*] Bernard Amadon,[†] Yves-Patrick Pellegrini, and Christophe Denoual

CEA, DAM, DIF, Arpajon F-91297, France

The mechanism of the α-ϵ transition in iron is reconsidered. A path in the Burgers description of the bcc/hcp transition, different from those previously considered, is proposed. It relies on the assumption that shear and shuffle are decoupled and require some peculiar magnetic order, different from that of α and ϵ phases as found in density-functional theory. Finally, we put forward an original mechanism for this transition, based on the successive shuffle motion of layers, which is akin to a nucleation-propagation process rather than to some uniform motion.

I. INTRODUCTION

The bcc-hcp transition in iron has recently been the subject of intense experimental[1–4] and theoretical[5–13] work. At room temperature and pressure, α-iron is a bcc metal with ferromagnetic (FM) order. Upon pressure, iron exhibits a phase transition at $\simeq 13$ GPa to a hcp structure[14–16] with no magnetic order.[17] The hysteresis at the transition is large,[18] and as pressure is changed, the transformation occurs rapidly, suggesting that the transition is nondiffusive and martensitic. A recent paper underlines the importance of antiferromagnetic (AFM) fluctuations in hcp ϵ-iron.[4]

In order to describe α-iron from an *ab initio* point of view, dynamical mean-field theory[12,19] in combination with density-functional theory (DFT) or other advanced schemes[13] have been used. In particular, the localization of electrons in the nonbonding e_g state but not in the bonding t_{2g} state is a key point[19] for understanding paramagnetic bcc iron. However, DFT *ab initio* techniques alone can handle FM bcc iron and the thermodynamical fundamentals of the $\alpha \rightarrow \epsilon$ transition:[20] The generalized gradient approximation (GGA) correctly captures the basic Stoner mechanism for the reduction in magnetism, under the increase in atom coordination during the $\alpha \rightarrow \epsilon$ transition, as well as the larger spin polarization of e_g orbitals with respect to t_{2g} in the α phase.

The $\alpha \rightarrow \epsilon$ transition can be viewed[21] as combining an anisotropic compression (shear) in the (100) direction of the bcc with a shuffle in the (011) plane, that corresponds to a zone-boundary transverse phonon mode (see, e.g, Ref. 5). Due to its martensitic nature, the transformation is triggered above the thermodynamical threshold, i.e., when the α and ε enthalpies are equal, which appears above $\simeq 10$–13 GPa,[5,7,9] as computed in the GGA.

However, its *ab initio* description is debated. Although the broad outline of the transition has been settled, a detailed description faces the problem of accurately computing the relevant energy barrier. Ekman *et al.*[5] demonstrated that the transition is first-order with no dynamical precursors and that it is caused by the effect of pressure on the magnetism of iron. Johnson and Carter[7] have shown that a minimization with respect to shuffle and shear, considered as independent variables, leads to a cusp in the energy profile with a particularly low-energy barrier. This pathway imposes a discontinuity of the shuffle displacement at no additional energetic cost. Rejecting this possibility, Liu and Johnson[9] stated that shuffle and shear are coupled and cannot be minimized separately. Still, the barrier energy found this way is too high—within

the range of pressures for which the transition is expected to occur—to permit the transformation.[6] No mechanism, allowing for a transformation with a reasonable energy barrier, has been proposed.

Investigations have established the role of complex magnetic structures for some transition paths of the $\alpha \rightarrow \gamma$ (Refs. 10, 22 and 23) and $\alpha \rightarrow \epsilon$ transitions,[6] e.g., for ϵ-Fe spin, spiral states have the same energy as AFM structures.[8] Yet, no study has been carried out on the effects of magnetic ordering on the pathway of the bcc-hcp martensitic phase transition.

As to the kinetics of the transition, no intermediate states were detected in experiments on the nanosecond time scale,[24] which suggests that the transformation is very rapid and probably propagates at near sound velocity. Moreover, it recently has been shown that, for cobalt, the transition occurs through microstructural avalanches.[25] Such behavior implies that the transition is not of the military type but instead involves localized transformation events. No such possibility has been considered yet for iron.

In this paper, we propose (Sec. II) an alternative description of the path for the $\alpha \rightarrow \epsilon$ transition within the Burgers mechanism. Second, using GGA calculations, we show the importance of AFM order to describe the energetics of this path (Sec. III A). Third, and this is our main result, we emphasize (Secs. III B and III C) that the shuffle mechanism could occur layer after layer in a nonsimultaneous way, thus, bridging the gap between the low-energy pathway of Ref. 7 and a description of the transition without any discontinuity in displacement.[9]

II. COMPUTATIONAL SETUP AND METHODOLOGY

The two-atom unit cell is replicated four times in the $(001)_{hcp} \parallel (110)_{bbc}$ direction into an eight-atom supercell with periodic boundary conditions (PBCs). The unit cell is represented in Fig. 1 with lattice vectors $\vec{R}_1$, $\vec{R}_2$, and $\vec{R}_3$. Three parameters are necessary to determine the unit cell: the angle α, the value of $c = R_2/4$, and the value of R_1. Three macroscopic quantities can be used to compute them: the volume, the $c/a = R_2/(4R_3)$ ratio, and the shear ϵ. In our paper, the volume, namely, 71.5 bohr^3/atom, is such that hcp and bcc energies coincide. The c/a ratio is kept constant and equal to $\sqrt{8/3} \simeq 1.633$, which is the value in the bcc structure and in the ideal hcp compact structure. The shear is defined by $\epsilon = (2\sin\alpha - \frac{2}{\sqrt{3}})/(1 - \frac{2}{\sqrt{3}})$ and is equal to 0 and 1,
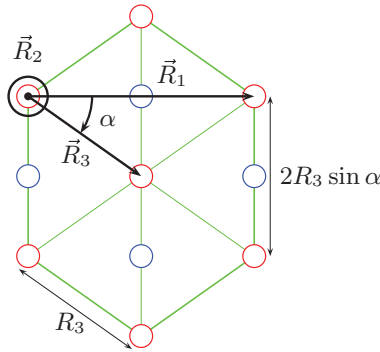
FIG. 1. (Color online) Scheme of the $(001)_{hcp} \parallel (110)_{bcc}$ plane in the bcc configuration. The vectors $\vec{R}_1$, $\vec{R}_2$, and $\vec{R}_3$ define our simulation cell. The red atoms and blue atoms lie in two different planes (see Fig. 2). $\vec{R}_2$ is perpendicular to $\vec{R}_1$ and $\vec{R}_3$, and $R_2 = 4c$. The shear is defined by $\epsilon = (2\sin\alpha - \frac{2}{\sqrt{3}})/(1 - \frac{2}{\sqrt{3}})$. In bcc, $2\sin\alpha = \frac{2}{\sqrt{3}}$, and $\epsilon = 0$. In hcp, $2\sin\alpha = 1$, thus, $\epsilon = 1$. From this definition, conservation of volume ($R_2 R_1 R_3 \sin\alpha = V$), conservation of $\frac{c}{a}$ ($= \frac{R_2}{4R_3} = \sqrt{\frac{8}{3}}$), and the geometric relation $2R_3 \cos\alpha = R_1$, give $\vec{R}_1$, $\vec{R}_2$, and $\vec{R}_3$ as a function of the value of the shear.

respectively, in the bcc and the hcp structures. For each value of the shear, we computed the energy for three values of the c/a ratio, namely, 1.605, $\sqrt{8/3} \simeq 1.633$, and 1.668 to check that the sheared bcc structure is stable with respect to a change in c/a and that $c/a = \sqrt{8/3}$ is close to the minimum. The results are insensitive to the small difference between this value and the true minimum. Finally, the shuffle η is proportional to the distance of one blue atom between its position during the transition (see Fig. 2) and the reference position in bcc.

We focus our paper on the shuffle part of the Burgers mechanism. Because of the different physical time scales involved,[7] we assume that the lattice shear deformation mode (ϵ) and the shuffle mode (η) are uncoupled in such a manner that, with respect to shear, shuffle is instantaneous. Volume and c/a ratio are, thus, kept constant during the shuffle. The path proposed in Ref. 7 is defined by the equality of the energies of the sheared bcc and hcp phases. In Ref. 7, however, the energetics of the shuffle is not explored. On the other hand, Liu and Johnson[9] couple shear and shuffle modes. Their path is schematically represented in black in Fig. 2. In this figure, the shear (ϵ_1) is fixed to half the value necessary to go from the bcc α phase to the hcp ϵ phase. It is the shear at the transition state computed by Ekman *et al.*[5] at constant volume. This choice guarantees that the shuffle mode goes through the transition state (TS) of Ref. 5 and corresponds to the energetically most favorable path, represented in solid red in Fig. 2.

In this paper, we are concerned by the shuffle mechanism along the BC line (see letters in Fig. 2). Since the shuffle of a large number of atoms can be described in several different ways, our aim is to understand whether the shuffle of all the layers is simultaneous or not.

A. Simultaneous shuffle

Let us first consider simultaneous shuffle (S). By $A\bar{A}A\bar{A}A\bar{A}A\bar{A}$, we denote the stacking of the eight atoms in the bcc-sheared phase, and by $B\bar{B}B\bar{B}B\bar{B}B\bar{B}$, we denote their stacking in the hcp-sheared phase. In this notation, A and $\bar{A}$,
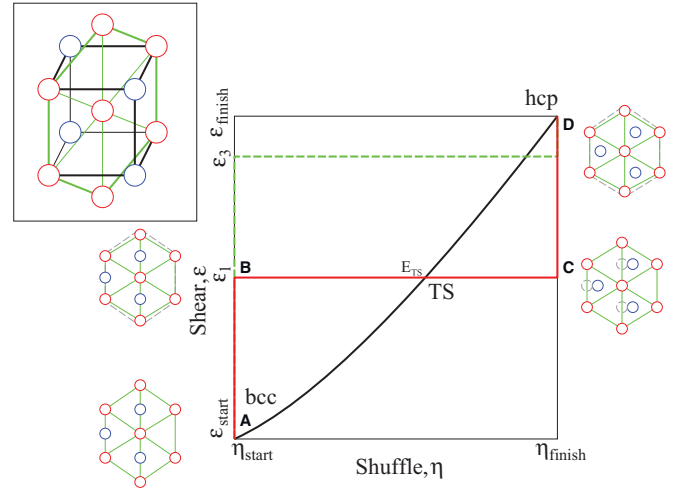

FIG. 2. (Color online) Sketch of possible paths for the bcc/hcp transition in the shear shuffle plane. TS is the transition state, and the black line corresponds to the lowest pass to go from the bcc valley to the hcp valley. The red and green lines are the transition paths that are studied in Fig. 4 (see also text). $\epsilon_1 = 0.5$, and $\epsilon_3 = 0.875$.

and B and $\bar{B}$, correspond to atoms in the bcc- or hcp-like configurations, respectively. The atoms in the A and $\bar{A}$ layers have 8 neighbors, whereas, atoms in the B and $\bar{B}$ layers have 12 neighbors. During the simultaneous shuffling of all four atoms of the $\bar{A}$-type layer into a $\bar{B}$-type layer, A-type layers are transformed into B-type layers. The transformation is, thus, $A\bar{A}A\bar{A}A\bar{A}A\bar{A} \rightarrow B\bar{B}B\bar{B}B\bar{B}B\bar{B}$ [Fig. 3(b)].
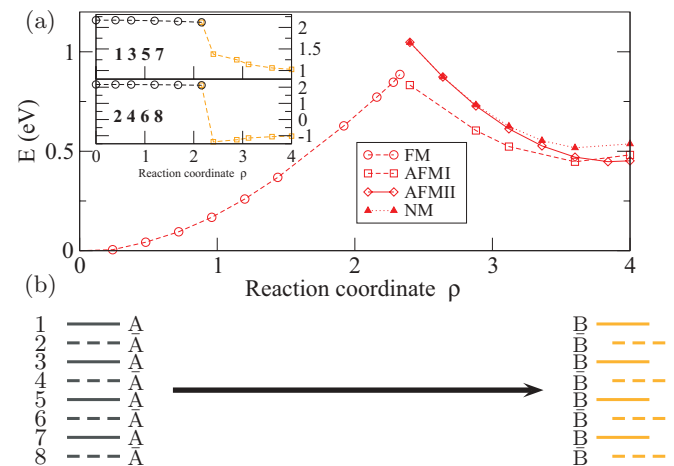

FIG. 3. (Color online) (a) Total energy for the simultaneous shuffle S_1 computed for FM, AFMI, AFMII,[31] and nonmagnetic (NM) configurations. S stands for simultaneous, and the index 1 refers to the shear ϵ_1 (see Fig. 2). The energy is given for a supercell of eight atoms to allow for an easy comparison with Fig. 4. (b) Stacking of the layers during the transition. In black, the A and $\bar{A}$ layers. In orange, the B and $\bar{B}$ layers. The black (respectively, orange) color, thus, indicates that the first shell of neighbors is bcc- (respectively, hcp-) like. In the inset, the evolution of the magnetic moment for the eight atoms during the FM $\rightarrow$ AFMI transition.
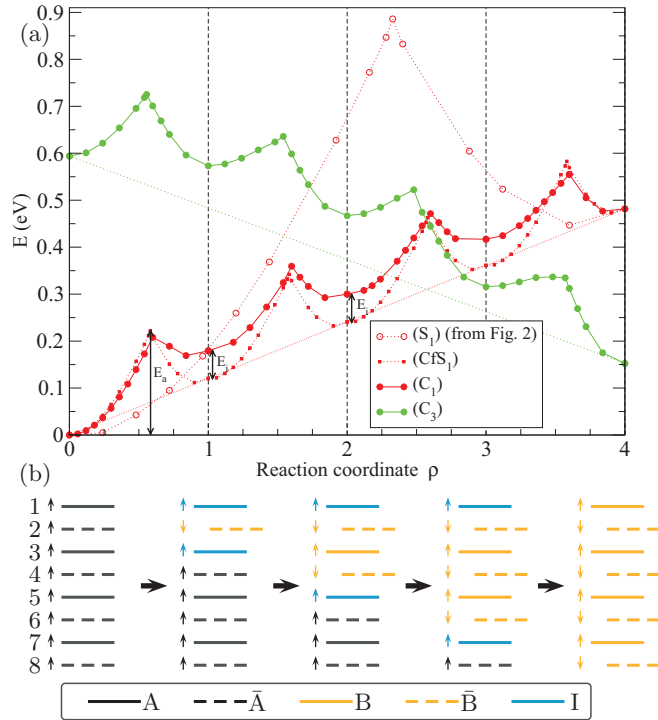
FIG. 4. (Color online) (a) Comparison of energies for three different shuffling mechanisms (for a shear of $\epsilon_1 = 0.5$). (S_1) is the simultaneous shuffling of all atoms. (CfS_1) stands for "consecutive from simultaneous," a hypothetical mechanism that corresponds to consecutive shuffles within an assumption of independent layers (interactions neglected), computed with the energies of mechanism S_1 (see text). (C_1) is the true energy computed when layers shuffle in a consecutive way (interactions included). E_i and E_a, respectively, represent the interface energy and the activation energy for the first shuffle (see text). (C_3) is the energy for the consecutive shuffling of the atoms for a shear of $\epsilon_3 = 0.875$. (b) Layer stacking during consecutive shuffling: in blue, layers in which the first atomic shell is intermediate between the bcc and the hcp environments. Arrows indicate the sign of the magnetic moment in each layer as described in Fig. 5.

B. Consecutive shuffle

Consider next the consecutive individual shuffle of layers (C), schematically represented in Fig. 4(b). First, we compute the individual shuffling of layer 2 from $\bar{A}$ to $\bar{B}$. It corresponds to the transformation $A\bar{A}A\bar{A}A\bar{A}A\bar{A} \rightarrow I\bar{B}IA\bar{A}A\bar{A}$. Due to the PBCs, this creates intermediate (I) configurations for the first and third layers. It corresponds to an atom layer sandwiched between one $\bar{B}$ and one $\bar{A}$ layer. Their local environment is, thus, neither bcc nor hcp.

In a second step, starting from the latter configuration, we study the shuffling of the second layer up to the new configuration $I\bar{B}B\bar{B}IA\bar{A}A$. During this transformation, the fourth layer shuffles from configuration $\bar{A}$ to configuration $\bar{B}$. Thus, the third layer now has a full hcp-like configuration around it and now is, thus, labeled B. The process can be pursued until all layers have shuffled.

C. Computational details

We use the projector wave augmented[26] implementation[27] of ABINIT (Ref. 28) in the GGA PBE approximation of

DFT. Atomic data include $3s$ and $3p$ semicore states,[26] the cutoff radius is 2.0 a.u., the energy cutoff for the plane-wave expansion is 20 Ha, and the convergence criterion for the charge-density residual is 10^{-9}. With these atomic data, results of Ref. 27 are reproduced. A $18 \times 4 \times 26$ special k-point mesh[29] and a Gaussian smearing of 5.10^{-4} Ha for electronic occupations[30] are used in order to obtain a good estimate of the energetic and magnetic properties.

III. RESULTS

A. Simultaneous shuffle

Energies for the simultaneous mechanism are displayed in Fig. 3(a). The reaction coordinate (ρ) is taken proportional to the shuffle (η) of the supercell atoms and varies from 0 (bcc like) to 4 (all atoms in a hcp-like environment). Near equilibrium ($\rho = 0$), the energy increases quadratically as expected. The curve exhibits a cusp at 60% shuffle amplitude due to a change in magnetism from FM to AFMI.[31] During this transition, the magnetic moment—reproduced in the inset of Fig. 3—changes abruptly from $2.2 \mu_B$/atom to $1.1 \mu_B$/atom in agreement with Ref. 6 where, however, AFMI order was not considered. This confirms the importance of magnetism for this transition:[5–7,9] Without any change in magnetism, the transition would not occur. In the rightmost part of the curve, the energy decreases to a local minimum corresponding to a deformed hcp phase. We computed the same curve with a cell of four atoms allowing for the creation of AFMII order.[31] We find, in agreement with Refs. 32 and 8, that AFMII is more stable for the hcp structure ($\rho = 4$) compared to AFMI. However, and interestingly, we also find that past the cusp, the AFMI structure is more stable than the AFMII. This highlights the important role of complex magnetism for the DFT description of the transition path and not only for the stable structure.[5] A complete study of magnetism, especially noncollinear, lies beyond the goal of our paper. We, nevertheless, show that an AFMI description of the transition path is particularly adapted to the present case. We call $E^{S_1}(\rho)$ the combination of the FM and AFMI curves. The energy profile qualitatively agrees with previous results, involving a smaller unit cell with two atomic layers (Figs. 5 and 6 of Ref. 5) even if Ekman *et al.* have considered a NM ground state for the hcp phase and the PW91 GGA functional.

B. Consecutive shuffle

Energy plots associated with the consecutive mechanism are drawn in Fig. 4(a). From $E^{S_1}(\rho)$, one can trivially compute the energy of shuffle per atom and, thus, can simulate the consecutive motion of four layers under the assumption that the energy for the shuffling of only one layer is equal to that for shuffling all layers divided by the number of layers. This approximation would be correct if there were no interactions between layers. For this mechanism, because all atoms are not shuffling at the same time, ρ describes the consecutive shuffling of all the layers. Formally, from value $n - 1$ to value n, $[\rho - (n - 1)]$ is, thus, proportional to the displacement of the atoms of the nth layer. As a consequence, for $\rho = 0$ and $\rho = 4$, whatever the mechanism, all atoms are in the same positions. The expression for $E^{CfS}(\rho)$ between $n - 1$ and n is

as follows:

$$E^{\mathrm{CfS}}(\rho) = \frac{E^S\{4[\rho-(n-1)]\}}{4} + (n-1)\frac{E^S(\rho=4)}{4}.$$

As a consequence, $E^{\mathrm{CfS}}(0)$, $E^{\mathrm{CfS}}(1)$, $E^{\mathrm{CfS}}(2)$, $E^{\mathrm{CfS}}(3)$, and $E^{\mathrm{CfS}}(4)$ lie on the same line (dashed red in Fig. 4). Trivially, this mechanism reduces the total energy barrier: In Fig. 4, the energy barrier $E^{\mathrm{CfS}_1}(\rho \simeq 3.53) - E^{\mathrm{CfS}_1}(\rho=0)$ is lower than the energy barrier $E^{\mathrm{S}_1}(\rho \simeq 2.30) - E^{\mathrm{S}_1}(\rho=0)$. Finally, the third curve (E^{C_1}) corresponds to the explicit calculation of the consecutive motion of four layers.

C. Discussion

We focus next on the comparison between the model of independent layers (CfS$_1$) and the true calculation (C$_1$). The two curves show the same main tendencies with four energy barriers corresponding to the shuffling of the four atoms and three metastable structures corresponding to the shuffling of only one, two, or three layers ($\rho = 1$–3). However, the energy of the three metastable configurations (for $\rho = 1$–3) differs by only $E_i = E^{\mathrm{C}_1}(1) - E^{\mathrm{CfS}_1}(1) = 60$ meV and is, thus, a constant independent of the number of shuffled layers. This suggests that E_i comes from the two interfaces (in blue in Fig. 4) between shuffled and unshuffled layers. The number of such interfaces is constant and independent of the number of layers.

To assess the electronic origin of these interface energies, Fig. 5 represents the evolution of the d-magnetic moment for the eight layers in the supercell as a function of ρ. The transition goes along with a progressive change in magnetism in which each successive layer shuffle, from the bcc- to the hcp-like configuration, involves local jumps from FM to AFMI. Indeed, after plane number 2 is translated, there is a local AFMI order around this layer. When plane number 4 is translated, AFMI order expands over five layers, and
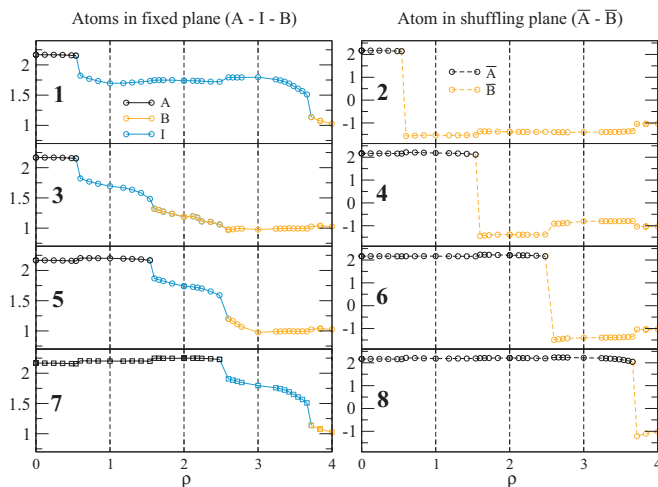
so forth. Also, the local moments strongly depend on local coordination, in agreement with the generalized Stoner mechanism for the appearance of magnetism as a function of bandwidth.[5] For example, when the fourth atom goes from a bcc-like local configuration to a more compact hcp-like local configuration, its local moment changes from $2.2\mu_B$ to $-1.1\mu_B$ with no substantial difference with the simultaneous mechanism. At the same time, the moment of the neighboring atom 5 changes from $2.2\mu_B$ to $1.7\mu_B$ only because atom 5 now has a local environment intermediate between the hcp and the bcc. Once atom 6 has moved, atom 5 ends up (for $\rho = 3$) with a full hcp-like local environment and a moment of $1.1\mu_B$. This demonstrates: (i) the absolute correlation between magnetism and total energy in the transition and (ii) the link between interfacial energy and layers with intermediate local moment and coordination. The interfacial energy only depends on the number of interfaces, which is constant in the present paper. Remarkably, energy barriers are not shifted by this interfacial energy.

For $\epsilon_1 = 0.5$, one notices that the energy progressively increases for all the metastable states up to the final energy gain of -0.5 eV. An additional calculation is performed for a shear of $\epsilon_3 = 0.875$ (green lines in Figs. 2 and 4). The resulting energy exhibits the same characteristics as for $\epsilon_1 = 0.5$ and notably an interface energy of 100 meV but with an overall gain of $+0.45$ eV after the shuffle. For $\epsilon_3 = 0.875$ and only around $\rho = 3$, a new magnetic order—not stable for $\epsilon_1 = 0.5$—diminishes the interface energy to 52 meV. It embodies both FM and AFM interactions between the layers and highlights the energetic proximity of several magnetic orders. Further studies, with larger supercells, would be necessary to study this magnetic order, but this is not the goal of the present paper.

Two shear thresholds for the bulk transformation can be estimated. A simple linear interpolation between the shuffle curves C_1 and C_3 produces the following energy for a shear ϵ_2 such that $\epsilon_1 \leqslant \epsilon_2 \leqslant \epsilon_3$ and the shuffle ρ,

$$E(\rho,\epsilon_2) = E^{\mathrm{C}_1}(\rho) + \frac{E^{\mathrm{C}_3}(\rho) - E^{\mathrm{C}_1}(\rho)}{\epsilon_3 - \epsilon_1}(\epsilon_2 - \epsilon_1).$$

A lower-nucleation-threshold (LT) shear $\epsilon_2^{\mathrm{LT}} \simeq 0.7$ is defined as the shear above which the gain $E(\rho=0,\epsilon_2) - E(\rho=4,\epsilon_2)$ becomes positive. To complete the transformation, the interface energy has to be overcome for the first layer only, leading to shuffling of subsequent layers at no additional cost. For a large number of layers, thermodynamical equilibrium, thus, drives the transition to completion. Also, an upper-nucleation-threshold (UT) shear of $\epsilon_2^{\mathrm{UT}} \simeq 0.84$ is estimated from the linear interpolation. It is defined as the shear above which the gain $E(\rho=0,\epsilon_2) - E(\rho=1,\epsilon_2)$ for the first metastable state becomes positive. Above this shear, even the first shuffle occurs at no energy cost. Then, all subsequent shuffles are strongly favored, possibly leading to propagation and to a global transition.

Consequences on the kinetics of the α-ϵ transition are as follows. Shuffle can be viewed as a thermally activated kinetic process due to vibrations of atoms.[5,7,9] As emphasized above, the energy barrier per atom E_a, which defines the activation energy, is independent of the interfacial energy so

FIG. 5. (Color online) Evolution of the local magnetic moment for the eight atoms of the supercell as a function of the reaction coordinate ρ. The black, orange, and blue colors approximately depict the bcc, hcp, and mixed bcc/hcp values for the magnetic moment. The atom numbering is related to Fig. 4. Atoms 1, 3, 5, 7 belong to the A layers, and atoms 2, 4, 6, 8 are successively moving from an $\bar{\mathrm{A}}$-type layer to a $\bar{\mathrm{B}}$-type one.

that the shuffle of a single layer has, thus, no supplementary activation cost. In this perspective, the above provides an alternative mechanism for the transition in which the bulk shuffle transformation nucleates from one single shuffle event, possibly initiated by some initial shear ϵ_2, such as, e.g., in a shock wave. This mechanism considerably reduces the amount of energy needed to trigger the transformation, the dimensionality of the nucleation process being reduced from 3 to 2.

In order to describe a transition corresponding to a shuffle for a domain, a complete thermodynamical description of this mechanism would be necessary. This would require relaxing atoms after each shuffle and is beyond the scope of our paper.

IV. CONCLUSION

In conclusion, we utilize the fact that shuffle—or optical-phonon mechanism—and macroscopic compression —shear—have, in general, different time scales, which allows for their decoupling. This is true for iron but also for other systems, such as Zr, Ba, or related transitions, such as Pu.[33] Second, in iron bcc-hcp transition, we show that the transition path description requires some peculiar magnetic order different from the magnetic order of equilibrium phases. Third, we highlight a new mechanism for this transition based on the successive shuffle motion of layers. It indicates that each layer itself could move by developing "shuffle dislocations" in a manner akin to slip motion in plasticity. Our paper suggests that detailed investigations of nucleation mechanisms would be required to resolve the frontier between the military and the thermally activated characters of solid-solid phase transitions.

*Present address: Institut für Theoretische Physik und Astrophysik, Christian-Albrechts-Universität zu Kiel, Leibnizstrasse 15, Kiel D-24098, Germany.

†bernard.amadon@cea.fr

[1] F. M. Wang and R. Ingalls, Phys. Rev. B **57**, 5647 (1998).

[2] J. Hawreliak, J. D. Colvin, J. H. Eggert, D. H. Kalantar, H. E. Lorenzana, J. S. Stölken, H. M. Davies, T. C. Germann, B. L. Holian, K. Kadau et al., Phys. Rev. B **74**, 184107 (2006).

[3] O. Mathon, F. Baudelet, J. P. Itié, A. Polian, M. d'Astuto, J. C. Chervin, and S. Pascarelli, Phys. Rev. Lett. **93**, 255503 (2004).

[4] A. Monza, A. Meffre, F. Baudelet, J.-P. Rueff, M. d'Astuto, P. Munsch, S. Huotari, S. Lachaize, B. Chaudret, and A. Shukla, Phys. Rev. Lett. **106**, 247201 (2011).

[5] M. Ekman, B. Sadigh, K. Einarsdotter, and P. Blaha, Phys. Rev. B **58**, 5296 (1998).

[6] M. Friák and M. Šob, Phys. Rev. B **77**, 174117 (2008).

[7] D. F. Johnson and E. A. Carter, J. Chem. Phys. **128**, 104703 (2008).

[8] R. Lizárraga, L. Nordström, O. Eriksson, and J. Wills, Phys. Rev. B **78**, 064410 (2008).

[9] J. B. Liu and D. D. Johnson, Phys. Rev. B **79**, 134113 (2009).

[10] S. V. Okatov, A. R. Kuznetsov, Y. N. Gornostyrev, V. N. Urtsev, and M. I. Katsnelson, Phys. Rev. B **79**, 094111 (2009).

[11] P. Tolédano, H. Katzke, and D. Machon, J. Phys.: Condens. Matter **22**, 466002 (2010).

[12] I. Leonov, A. I. Poteryaev, V. I. Anisimov, and D. Vollhardt, Phys. Rev. Lett. **106**, 106405 (2011).

[13] J. Sánchez-Barriga, J. Fink, V. Boni, I. Di Marco, J. Braun, J. Minár, A. Varykhalov, O. Rader, V. Bellini, F. Manghi et al., Phys. Rev. Lett. **103**, 267203 (2009).

[14] T. Takahashi and W. A. Bassett, Science **145**, 483 (1964).

[15] R. Clendenen and H. Drickamer, J. Phys. Chem. Solids **25**, 865 (1964).

[16] H.-K. Mao, W. A. Bassett, and T. Takahashi, J. Appl. Phys. **38**, 272 (1967).

[17] G. Cort, R. D. Taylor, and J. O. Willis, J. Appl. Phys. **53**, 2064 (1982).

[18] P. M. Giles, M. H. Longenbach, and A. R. Marder, J. Appl. Phys. **42**, 4290 (1971).

[19] A. A. Katanin, A. I. Poteryaev, A. V. Efremov, A. O. Shorikov, S. L. Skornyakov, M. A. Korotin, and V. I. Anisimov, Phys. Rev. B **81**, 045117 (2010).

[20] L. Stixrude, R. E. Cohen, and D. J. Singh, Phys. Rev. B **50**, 6442 (1994).

[21] W. G. Burgers, Physica **1**, 561 (1934).

[22] L. Tsetseris, Phys. Rev. B **72**, 012411 (2005).

[23] Y. Tsunoda, J. Phys.: Condens. Matter **1**, 10427 (1989).

[24] J. A. Hawreliak, B. El-Dasher, H. Lorenzana, G. Kimminau, A. Higginbotham, B. Nagler, S. M. Vinko, W. J. Murphy, T. Whitcher, J. S. Wark et al., Phys. Rev. B **83**, 144114 (2011).

[25] C. Sanborn, K. F. Ludwig, M. C. Rogers, and M. Sutton, Phys. Rev. Lett. **107**, 015702 (2011).

[26] P. E. Blöchl, Phys. Rev. B **50**, 17953 (1994).

[27] M. Torrent, F. Jollet, F. Bottin, G. Zérah, and X. Gonze, Comput. Mater. Sci. **42**, 337 (2008).

[28] X. Gonze, B. Amadon, P.-M. Anglade, J.-M. Beuken, F. Bottin, P. Boulanger, F. Bruneval, D. Caliste, R. Caracas, M. Côté et al., Comput. Phys. Commun. **180**, 2582 (2009).

[29] H. J. Monkhorst and J. D. Pack, Phys. Rev. B **13**, 5188 (1976).

[30] M. Methfessel and A. T. Paxton, Phys. Rev. B **40**, 3616 (1989).

[31] AFMI is the AFM coupling of layers in the 0001 direction, whereas, AFMII is an AFM coupling inside the 0001 plane: See, e.g., Fig. 1 of Ref. 8.

[32] G. Steinle-Neumann, L. Stixrude, and R. E. Cohen, Phys. Rev. B **60**, 791 (1999).

[33] T. Lookman, A. Saxena, and R. C. Albers, Phys. Rev. Lett. **100**, 145504 (2008).